The Measured and Computed Performance of a 140–220GHz Schottky Diode Mixer

PETER H. SIEGEL MEMBER, IEEE, AND A. R. KERR, FELLOW, IEEE

Abstract—**In this paper, we compare the measured and theoretical performance of a room-temperature single-ended Schottky diode mixer in the WR-5 (140–220-GHz) waveguide band. Using the computer program GISSMIX, combined with measurements made on a 100× scale model of the WR-5 mixer, we have been able to predict the millimeter-wave mixer performance over a wide tuning range with unprecedented accuracy. In addition, we have examined the sensitivity of the mixer performance to various diode and mount characteristics. Our measured conversion loss and mixer noise temperature, single sideband, are 5.7 dB and 750 K at 180 GHz, and 5.7 dB and 500 K at 150 GHz, which we believe to be the best reported for a room-temperature mixer at these frequencies.**

I. Introduction

AT FREQUENCIES above 100 GHz, reported mixer performance varies widely from laboratory to laboratory, and in fact there is considerable variation among mixers produced in the same laboratory using diodes fabricated from the same semiconductor wafer. The reasons for these differences have never been adequately explained. In addition, few guidelines exist to aid researchers in their efforts to produce better mixer diodes, nor is there any clear understanding of the relationships between mixer performance and the diode mounting circuit at these frequencies. We have addressed these problems by using the computer program GISSMIX [1] to analyze a room-temperature single-ended Schottky diode mixer [2] in the WR-5 (140–220-GHz) waveguide band.

In an earlier study, Held and Kerr [3] analyzed a room-temperature mixer operating at ~100 GHz. We have refined and extended their work to ~200 GHz. Using measured diode and mount characteristics, we have been able to predict the performance of the WR-5 mixer over a wide tuning range with unprecedented accuracy. In addition, we have examined the sensitivity of the mixer performance to various diode and mount characteristics. The results of this study are presented in the hope that they may serve as a guide to future mixer designers.

II. Mixer Analysis

The computer program GISSMIX [1] performs complete large-signal, small-signal, and noise analyses on a mixer with known diode and mount characteristics. This program was used to analyze a WR-5 mixer containing a GaAs Schottky-barrier diode in the hope of gaining a better understanding of the factors affecting the mixer performance. A short summary of the computer analysis follows.

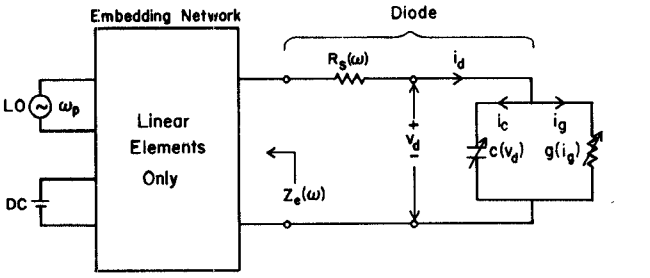

Fig. 1. The large-signal equivalent circuit of the mixer, used to determine the local oscillator current and voltage waveforms at the diode. The embedding network contains all the linear elements comprising the diode mount and source impedance.

The large-signal mixer equivalent circuit solved by the program GISSMIX is shown in Fig. 1. The embedding network, representing the waveguide mount, appears as a linear black box whose input impedances $Z_e(\omega)$ must be specified at the local oscillator (LO) and its harmonic frequencies (see Section III). The diode is modeled in the usual way by a varying conductance $g(i_g)$ shunted by a voltage-dependent capacitance $c(v_d)$. The series resistance $R_s(\omega)$ accounts for the resistance of the undepleted epitaxial layer and of the bulk semiconductor material. It is a function both of frequency and of diode geometry. The diode equivalent circuit is discussed further in Section IV.

GISSMIX solves the mixer equivalent circuit for the LO waveforms $v_d(t)$, $i_d(t)$, $c(t)$, and $g(t)$ using a form of the multiple reflection technique [4], described in detail in [5]. Although this nonlinear circuit algorithm is somewhat slower than other reported techniques [6], [7], it requires no initial guesses and has converged for all of the mixer circuits we have examined.

The small-signal analysis follows the methods of Held and Kerr [3] which are an extension of the original theory of frequency conversion given by Torrey and Whitmer [8]. The mixer is represented by a linear multifrequency multiport network in which there is one port for each sideband frequency, as shown in Fig. 2. In the analysis, a conversion admittance matrix is formed which relates the small-signal sideband currents and voltages at the diode. The elements of this matrix are derived from the Fourier coefficients of the large-signal diode conductance and capacitance waveforms. The conversion loss and mixer port impedances can

Manuscript received April 30, 1984. This work was performed while the authors were with the NASA/Goddard Institute for Space Studies, New York, NY.

The authors are currently with the National Radio Astronomy Observatory, Charlottesville, VA 22903.

0018-9480/84/1200-1579$01.00 ©1984 IEEE

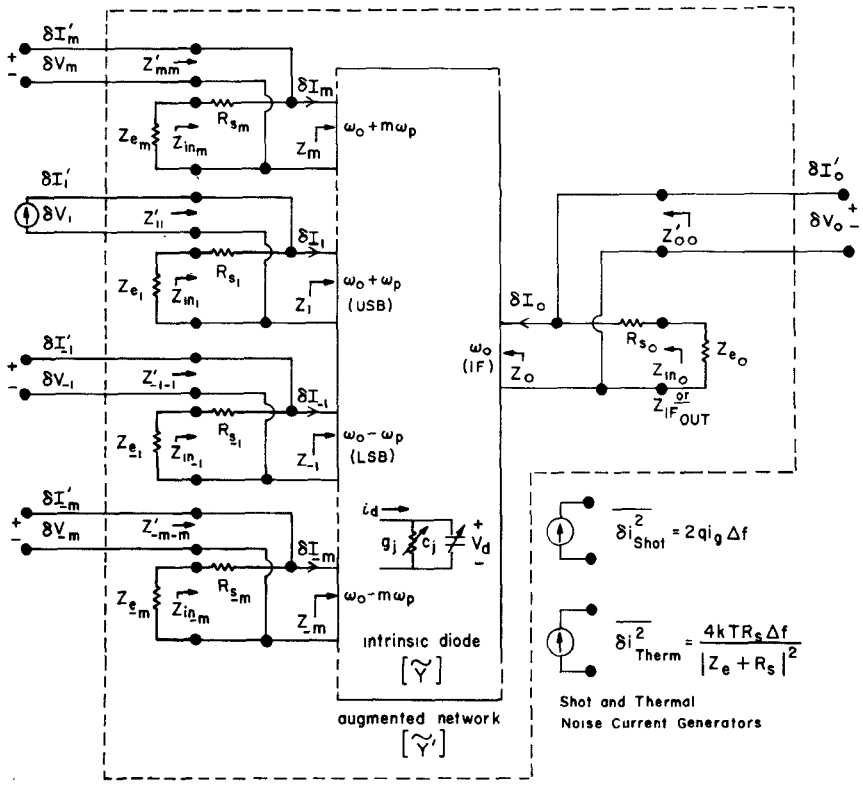

Fig. 2. The small-signal representation of the mixer as a multifrequency linear multiport network. δV_m and δI_m are the small-signal voltage and current components at sideband m (frequency $\omega_0 + m\omega_p$) at the intrinsic diode (the diode minus its series resistance). The conversion matrix $\tilde{Y}$ represents the pumped intrinsic diode, and the augmented network, represented by $\tilde{Y}'$, includes the sideband embedding impedances and diode series resistance. $\delta I'_{\pm 1}$ is the equivalent signal current generator which is connected at port ± 1 of the augmented network during normal mixer operation, the other ports being open circuited. In the noise analysis, equivalent shot and thermal noise current generators (shown in the lower right) are connected across each of the ports.

be determined from the admittance matrix and the embedding impedances of the diode mount at the various sideband frequencies. Note that for all the results presented here, an optimum intermediate frequency (IF) load impedance is assumed, i.e., the IF load impedance is conjugate matched to the IF output impedance.

The noise analysis is based on the matrix formulation of [3]. Two sources of noise are considered: shot noise from the current flow across the Schottky barrier, and thermal noise in the diode series resistance. The effects of lattice and intervalley scattering and hot electron noise were not included in the current work.

In the analysis, equivalent shot and thermal noise current generators are placed across the ports of the small-signal mixer equivalent circuit shown in Fig. 2. Correlation matrices are formed and evaluated for both shot and thermal noise sources. The shot noise correlation matrix has elements related to the Fourier coefficients of the diode conductance current, while the thermal noise correlation matrix depends only upon the diode series resistance and the embedding impedances at the sideband frequencies. The two matrices together yield the total output noise voltage from which the equivalent input noise temperature of the mixer can be calculated. Again, for the results given here, the IF load impedance is conjugate matched to the IF output impedance. For further details of the mixer analysis and a complete listing of the program GISSMIX, the reader is referred to [5].

In order to use GISSMIX for the analysis of the WR-5 mixer, the embedding impedances at the sideband and LO harmonic frequencies and the diode equivalent circuit parameters must be given. The methods used to determine these quantities are discussed in the next two sections.

III. Diode Mount Impedances

To perform an accurate mixer analysis, we must know the mount (embedding) impedances, as seen by the diode, at the LO harmonic and sideband frequencies. In most earlier mixer analyses, an assumption was made that the higher harmonic sidebands (those above the upper sideband) were short-circuited by the diode capacitance. This assumption is clearly inaccurate for many of the high-frequency mixer diodes in use today, whose mean capacitance over an LO cycle may be as low as a few femtofarads. In fact, we show in Section VII that, for our WR-5 mixer, the terminations at the second harmonic sidebands do significantly affect the mixer performance.

A theoretical computation of the embedding impedances of a realistic waveguide mixer is very difficult, and direct measurement is impractical for our WR-5 mixer. Therefore, a 100× scale model of the WR-5 mixer was constructed, and a technique described by Eisenhart and Khan

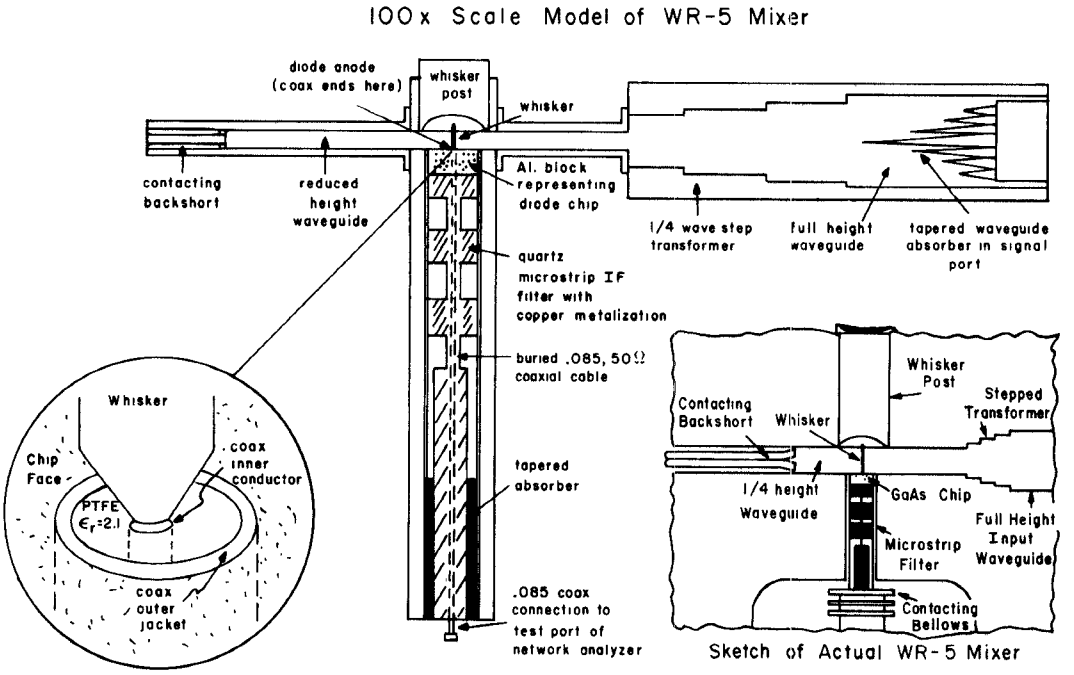

Fig. 3. A cross-sectional view of the 100× scale model of the WR-5 mixer used for obtaining the diode-embedding impedances. The inset at the left shows the region around the diode. A cross-sectional view of the actual WR-5 mixer is shown at the right.

[9] was used to measure the diode embedding impedances at the equivalent of 1-GHz intervals from 140 to 1320 GHz (the sixth harmonic of 220 GHz), for many different settings of the mixer tuning short circuit (backshort). In this way, the diode mount was characterized over the entire mixer operating range and for any desired intermediate frequency. A cross-sectional view of the 100× scale model mixer is shown in Fig. 3. Details of the actual WR-5 mixer and its design and construction are given in [2].

In the model, a small coaxial cable runs along the underside of the metalization of the mixer's low-pass microstrip filter structure and passes through the metal block representing the diode chip (see Fig. 3). The cable ends at the position normally occupied by the anode of the actual diode, and here the center conductor is brought into contact with a scaled version of the diode whisker. The opposite end of the cable (at the rear of the microstrip filter) is brought out to a network analyzer whose reference plane is adjusted to coincide with the anode of the diode. After correcting for small differences between the actual mixer and the scale model, the impedances measured on the network analyzer give the diode embedding impedances $Z_e(\omega)$ we are seeking.

Figs. 4 and 5 contain Smith Chart plots showing the measured diode embedding impedances (normalized to 50 Ω) as a function of mixer backshort position at the first six LO harmonic frequencies and the first three associated sideband pairs, for an IF of 4 GHz. The symbols on the plots indicate the embedding impedances which resulted in the lowest computed mixer conversion losses (see Section VI). Even when the mean diode junction capacitance is added in, the higher harmonic impedances are neither short- nor open-circuited, as has been assumed in many earlier mixer analyses. Also notice that, for the case of a 4-GHz IF as used here, there is a considerable difference between the the upper and lower sideband embedding impedances, which, as we show in Section VI, results in a marked difference in mixer performance at the two sidebands.

IV. Diode Equivalent Circuit

The Schottky diodes used in the WR-5 mixer are of the honeycomb type and were fabricated by R. J. Mattauch at the University of Virginia, Charlottesville. The substrate is composed of n-type GaAs and is silicon doped to a concentration of 2×10^{18} atoms/cm^3. The epitaxial layer is approximately 800 Å thick and has a doping concentration of 2×10^{17} atoms/cm^3. The anodes are electroplated gold with a platimun interface layer. They are ~ 2 μm in diameter and have a center to center spacing of ~ 4 μm. The diode chip itself is 0.005 by 0.009-in on the front face and 0.005 in thick with an ohmic contact at the rear.

The diode equivalent circuit parameters used in the mixer analysis program are shown in Fig. 6 and were obtained as follows.

i_g: We have assumed (and will later verify for the WR-5 mixer) that the diode conduction current i_g obeys the thermionic emission theory [10]: $i_g = i_s[e^{qv_d/\eta kT} - 1]$, with i_s being the diode saturation current, q the electronic charge, η the diode ideality factor, k Boltzmann's constant, and T the diode physical temperature. No account has been taken in the analysis of quantum mechanical tunneling [11], lattice and intervalley scattering [12], ballistic transport [13], or of very high-frequency effects, such as dielectric relaxation, plasma resonance, and charge carrier inertia [14], which may cause the current–voltage relationship to deviate from the form given here. The only evi-

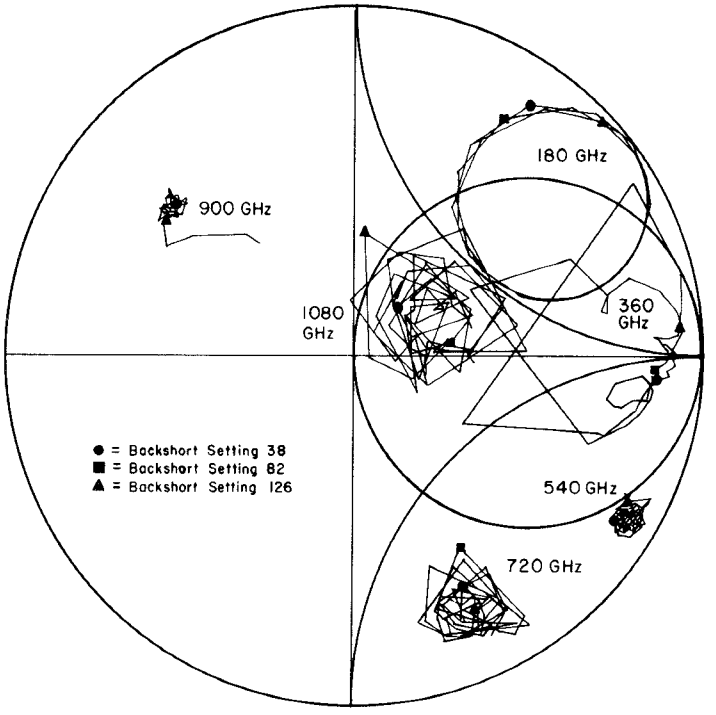

Fig. 4. A Smith Chart plot of the diode-embedding impedances (normalized to 50 Ω) as a function of backshort position for an LO frequency of 180 GHz and five higher harmonics. The plotted symbols indicate the three backshort positions at which the mixer had the lowest conversion losses (see Fig. 11).

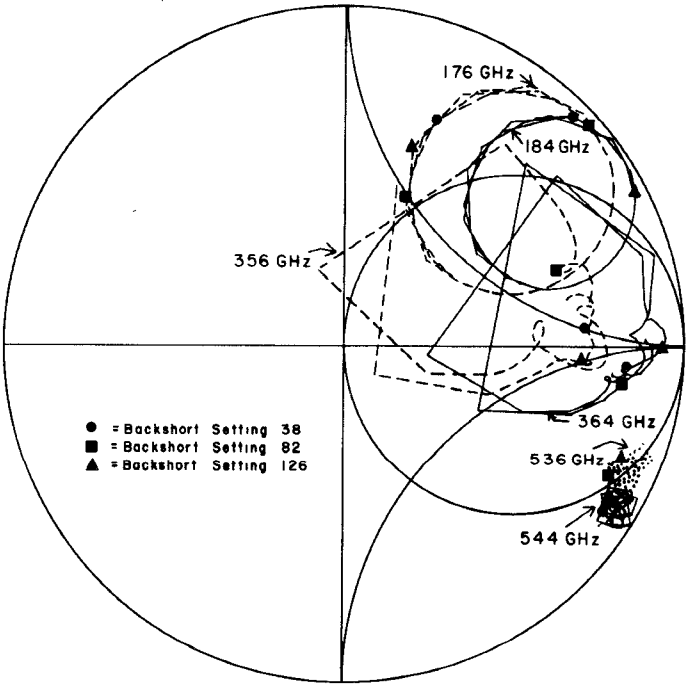

Fig. 5. A Smith Chart plot of the diode-embedding impedances (normalized to 50 Ω) at the first three harmonic sideband pairs, as a function of mixer backshort position. The LO frequency is 180 GHz and the IF is 3.95 GHz. As in Fig. 4, the plotted symbols indicate the three backshort positions at which the mixer had the lowest conversion losses (see Fig. 11).

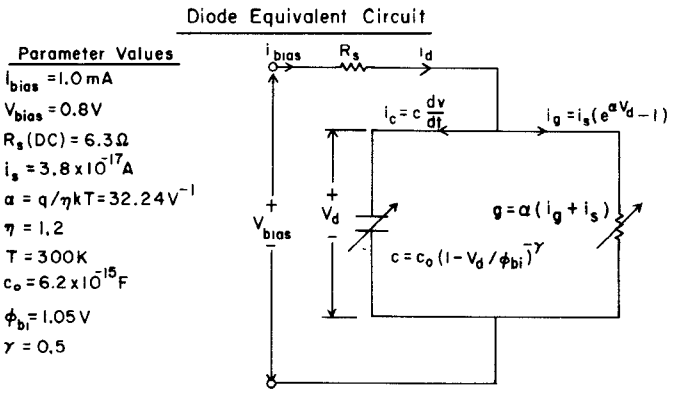

Fig. 6. The diode equivalent circuit with the derived parameter values used in the mixer analysis program.

dence we have that these effects are not strong in our diode at 200 GHz is the excellent agreement we have obtained between the computed and measured mixer performance (see Section VI).

i_s: The diode saturation current was obtained from the log $I-V$ curve by extrapolating v_d back to the I-axis. Little error is introduced if the saturation current is assumed to be independent of voltage, and a constant value of 3.8×10^{-17} amperes was used in the analysis.

η: The diode ideality factor was obtained from the slope of the log $I-V$ curve and was found to be 1.18 ± 0.02. η was then adjusted within these error limits to give a best fit between the measured and computed mixer performance. This fitting was necessary because of the extreme sensitivity of the computed mixer performance to variations in the value of η (with i_s held constant) and, as we will see in Section VI, is justified by the excellent agreement we were able to obtain between the measured and computed results over the whole of the mixer tuning range. A value for η of 1.20 was used in the computer program.

T: The physical temperature of the diode was taken to be 300 K. It has been suggested that the effects of lattice and intervalley scattering and hot electron noise may be approximated by a slight increase in the value of this quantity [3], although this was not found necessary in the present work.

$c(v_d)$: We have taken the usual form for the diode capacitance-voltage relationship in the computer program, that is: $c = c_0[1 - v_d/\phi_{bi}]^{-\gamma}$, where c_0 is the zero-bias junction capacitance, ϕ_{bi} is the built-in potential, and the exponent γ is a function of the doping profile, lying between 1/3 and 1/2.

c_0: The zero-bias junction capacitance c_0 was measured during the diode contacting procedure. The diode package capacitance is monitored with a Boonton model 75D 1-MHz capacitance bridge as the whisker is brought into contact with the anode. When contact is made, the junction capacitance is added in parallel with the parasitic capacitance and the reading jumps by an amount equal to c_0 (6.2 fF for our diode).

ϕ_{bi}: The value of the built-in potential (the potential difference from the conduction band edge to the asymptotic value of the barrier height) was obtained from mea-

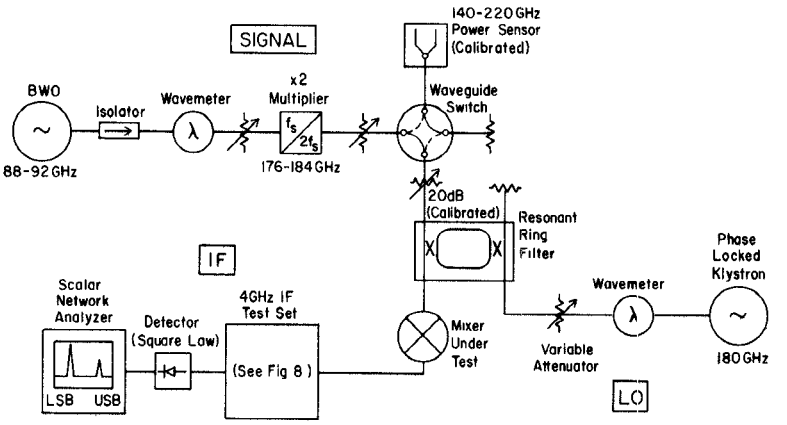

Fig. 7. The measurement test set used to determine the upper (USB) and lower (LSB) sideband conversion losses of the WR-5 mixer. The LO frequency is 180 GHz and the IF is 3.95 GHz. The IF test set gain and RF waveguide component losses are calibrated separately.

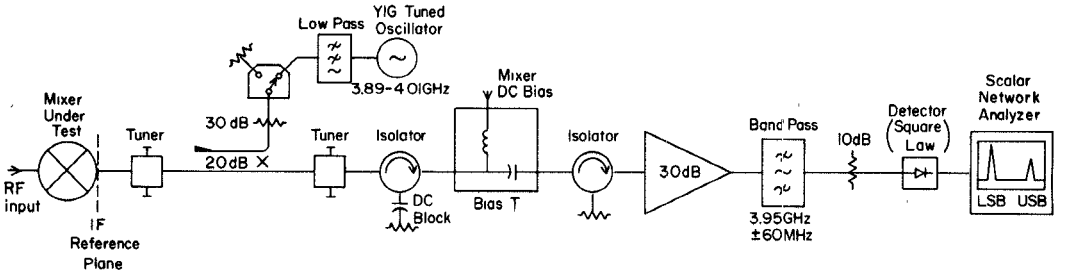

Fig. 8. The IF section of the conversion-loss test set. For the conversion-loss measurements, the switch is set on the 50-Ω termination. To measure the IF-port VSWR, the switch is set as shown. The left-hand tuner is adjusted to cancel the directivity error of the 20-dB coupler. The right-hand tuner is then adjusted to minimize the input VSWR of the test set with respect to 50 Ω, so the mixer is always connected to a 50-Ω IF termination. The second isolator is necessary to achieve sufficient isolation between the mixer-under-test and the IF amplifier.

surements made at the University of Virginia [15] on similar diodes and was taken to be 1.05 V.

γ: It is not practical to measure γ by the usual capacitance bridge technique because the test signal of the bridge is too large to allow an accurate reading of the capacitance in the voltage region over which the mixer diode normally operates. A value for γ of 0.5 was found to give the best fit between the measured and predicted mixer performance. In addition, we have assumed that γ is independent of voltage, which seems justified by the close agreement we have obtained between the measured and computed performance.

R_s: The diode series resistance at dc was determined in the usual way from the $\log I-V$ curve and was found to be 4.3 Ω. The effect of diode heating has been analyzed by Weinreb and Decker [16], and adds an additional 2 Ω to the value obtained from the dc $I-V$ curve. At high frequencies, the series resistance is increased by the skin effect, which contributes equal resistive and reactive components to R_s. The increase in R_s due to current flowing out from the anode along the surface of the diode chip was calculated using the formulation of Dickens [17]. The additional contribution from current flow down the side walls of the chip (to the ohmic contact at the rear) was computed by assuming a cylindrical geometry (see [5, appendix 2]). At 180 GHz, we calculated that the skin effect contributes 2.5 Ω to the dc value of R_s and, at the sixth harmonic (1080 GHz), the dc-series resistance was increased by roughly 7 Ω.

Finally, we have considered only shot and thermal noise in our analysis. The agreement we have obtained between the measured and the computed mixer performance indicates that, at least at room temperature, the contributions to the total noise from intervalley and lattice scattering and hot electron noise are small in our mixer.

V. Mixer Measurements

For comparison with the mixer analysis program, the performance of the WR-5 mixer was measured at 150 and 180 GHz over a wide range of tuning conditions. The parameters which were measured are the upper and lower sideband conversion losses, the single-sideband equivalent input noise temperature, the output noise-temperature ratio, and the voltage standing-wave ratio at the mixer's IF port referred to 50 Ω.

The upper and lower sideband conversion losses were determined from direct RF and IF power measurements using the test setup depicted in Fig. 7. The signal power incident at the mixer RF port was measured with a thermocouple-type power sensor (Anritsu model MP84B1) after reducing the attenuation in the calibrated attenuator (normally set to 20 dB for the measurements). Measurement error is due mainly to uncertainties in the power sensor calibration and to RF mismatch in the signal path. The resulting uncertainty in the final conversion-loss values was determined to be ± 1.0 dB. This was reduced to ± 0.5 dB by a double-sideband conversion-loss measurement using thermal RF noise sources (ambient and liquid nitrogen

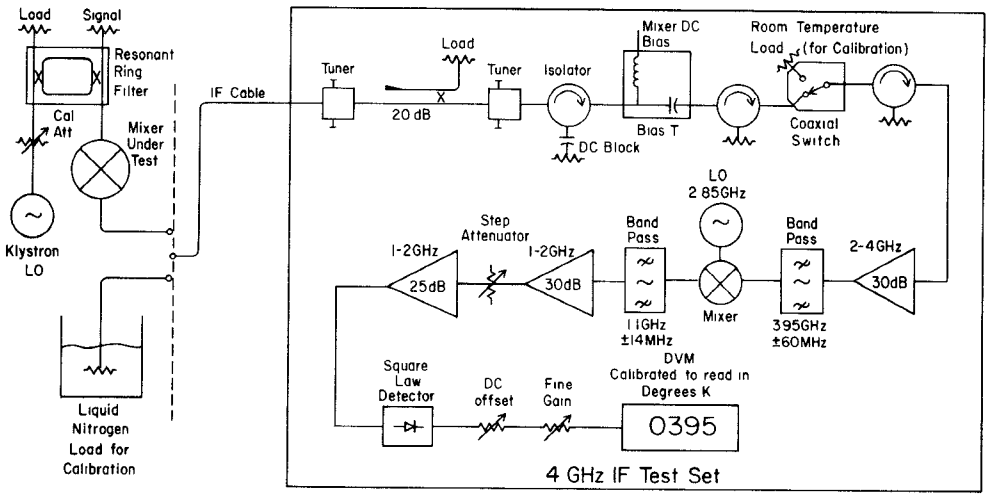

Fig. 9. A block diagram of the test set used for the mixer noise measurements. The system is similar to one described in [18]. The digital voltmeter (DVM) is calibrated to read in degrees by toggling the switch between the room-temperature load and the liquid nitrogen load at the end of the IF cable. With the mixer connected, the DVM indicates $t_r \times 290$ K (t_r is the output noise-temperature ratio of the mixer without any correction for IF mismatch). The directional coupler can be used if a separate measurement of the IF VSWR is desired.

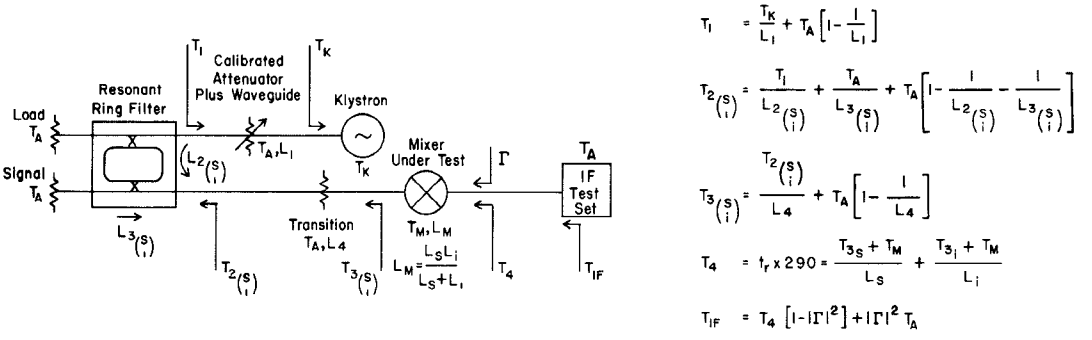

Fig. 10. The various contributions to the measured mixer output noise temperature T_{IF}. The attenuator is adjusted to obtain the desired rectified current in the diode. The equivalent input noise temperature of the mixer $T_M(dsb)$ can be found once the RF component losses have been measured. T_K represents the klystron sideband noise (see text). A subscript containing an s above an i in parentheses should be read as: at the signal and the image frequency.

temperature loads) with an RF radiometer/reflectometer similar to that of [18].

For comparison with the results of the mixer analysis program, the measured values of conversion loss must be corrected for mismatch between the mixer output port and the 50-Ω IF test set cable. The mismatch is determined during the conversion loss measurements using the test set depicted in Fig. 8. Low-level IF power from the YIG-tuned oscillator is injected, via a directional coupler, towards the output port of the mixer. The reflected power is measured with a scalar network analyzer connected at the output of the IF test set. This reading is then compared to a reference level taken with the IF port open circuited, yielding the voltage reflection coefficient at the output port of the mixer. The measured reflection coefficient is then used to derive the IF output VSWR and to obtain the conversion loss into a matched IF load. The two fine tuners in Fig. 8 are necessary to provide, simultaneously, a test set input VSWR <1.03 and an effective directivity for the coupler of >40 dB. When measuring mixers with high VSWR's, the errors introduced by these quantities can be substantial.

The double-sideband equivalent input noise temperature[1] $T_M(dsb)$ was measured with the test set shown in Fig. 9. The IF portion of the test set is calibrated using room-temperature and liquid nitrogen loads so that the digital voltmeter (DVM) reads in degrees. With the mixer connected, the DVM indicates $t_r \times 290$ K (t_r is the output noise-temperature ratio of the mixer without any correction for IF mismatch). The equivalent input noise temperature (double-sideband) is found by solving for $T_M(dsb)$ in the relationships given in Fig. 10 (the reflection coefficient and conversion losses at each mixer backshort setting having been determined previously).

It should be noted that, because of the finite attenuation of the resonant ring filter at the upper and lower sidebands, the output noise temperature measured on the DVM contains a small contribution from klystron sideband noise. To determine this extra noise term, we must perform an additional measurement which consists of plac-

[1]The single-sideband equivalent input noise temperature $T_M(ssb)$ can be found from $T_M(dsb)$ using: $T_M(ssb) = T_M(dsb)\,[1 + L_s/L_i]$, where L_s and L_i are the signal and image conversion losses, respectively.

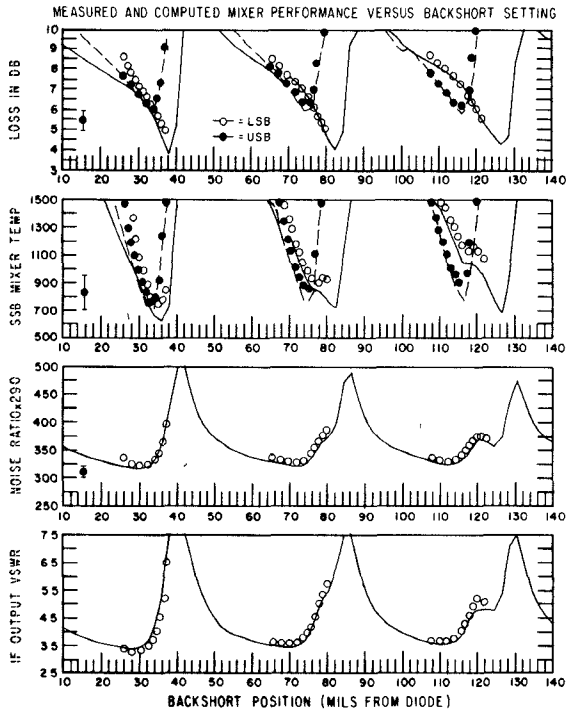

Fig. 11. A comparison of the measured (points) and computed (lines) mixer performance at 180 GHz. The output noise-temperature ratio (third graph) has been multiplied by 290 for convenience. Error bars are shown at the left.

ing the klystron (plus attenuator) directly at the RF port of the mixer. By combining the measured output noise with that obtained using the setup of Fig. 9, we are able to solve for the equivalent noise temperature of the klystron and to obtain the correct values of $T_M(dsb)$ and t_r (further details are given in [5]). Typically, for our klystrons, T_K ranged from 10000 to 14000 K and the additional contribution to $T_M(dsb)$ amounted to 10–15 K.

VI. Comparison of Measured and Computed Performance

The measured embedding impedances and the electrical properties of the diode were used in the mixer analysis program to compute the upper and lower sideband conversion loss, equivalent input noise temperature, output noise-temperature ratio, and the IF output VSWR at each of 66 backshort positions.[2] The results for an LO frequency of 180 GHz and a 4-GHz IF are shown superimposed on the measured values in Fig. 11 as functions of the mixer backshort position. The error bars shown on each diagram reflect the uncertainties of ± 0.5 dB in the conversion loss and ± 3K in T_{IF} (see Fig. 10). For all the points, the dc-bias voltage was fixed at 0.8 V and the incident LO power was adjusted until a rectified current of 1 mA flowed in the diode. Where no measured points appear, there was insufficient LO power available to obtain the required diode-rectified current.

[2]Note that at each backshort position a completely different set of impedances is presented to the diode requiring that the full mixer analysis be repeated.

The measured and computed results are in close agreement, except in the region where the backshort is very near to the diode. Here, differences between the backshorts in the actual mixer and the scale model, used for deriving the diode-embedding impedances (see Section III), may be significant because of evanescent mode coupling between the diode structure and the backshort when the spacing is small. Most of the discrepancy between the measured and computed input noise temperature is due to the uncertainty in the upper and lower sideband conversion losses. The output noise temperature ratio does not involve a separate measurement of the conversion loss at the two sidebands and, as a result, shows much better agreement with the computer analysis. Note that the upper and lower sideband performance differs markedly, emphasizing the importance of making measurements at both frequencies. The mixer performance was also computed and measured at 150 GHz (at the same 66 backshort settings) and similar agreement was obtained.

The excellent agreement between the measured and predicted mixer performance suggest that, in this mixer and under the prescribed operating conditions, the current flow is accurately described by the thermionic emission theory. The high-frequency effects described in [14], which may become significant in this mixer at the higher harmonics, do not have any measurable effect on the mixer performance. In addition, we see no significant excess noise from lattice and/or intervalley scattering. The results also justify our choices of η, ϕ_{bi}, and γ and suggest that the mixer analysis program might be useful in deriving more accurate values for these variables than can be determined by other measurement techniques.

Finally, we note that the measured noise temperature and conversion loss at 180 GHz are the best reported in the literature for a room-temperature Schottky diode mixer. At 150 GHz, our best measured mixer conversion loss and noise temperature (single-sideband) were 5.7 dB and 500 K, respectively.

VII. Sensitivity Analysis

Having demonstrated that the mixer analysis program correctly predicts the performance of the WR-5 mixer, we have used it to study the sensitivity of the mixer to various diode and mount characteristics. Fig. 12 summarizes the changes produced in the mixer performance at 180 GHz by varying nine different diode parameters, including the dc-bias voltage and rectified current. The first five parameters in the Table of Fig. 12 (I_{bias}, V_{bias}, R_s, c_0, and γ) can be adjusted more or less independently. However, the remaining quantities η, ϕ_{bi}, i_s, and T cannot be varied separately in practice. They are included in Fig. 12 to indicate the effect that uncertainties in these parameters will have on the computed mixer performance. In all instances, except those involving changes in V_{bias} and I_{bias}, the dc-bias voltage and diode-rectified current were fixed at 0.8 V and 1 mA, respectively. Each of the results given in Fig. 12 will be briefly discussed here and the reader is referred to [5] for additional details.

Diode Parameter	V_{bias}	I_{bias}	R_s	C_0	γ	η	ϕ_{bi}	i_s	T
Range	065-0 85V	05-2 0mA	3-12Ω	4-8fF	03-05	1 16-1 24	1 01-1 10	2-6x10^{-17}	295-310K
% Variation (Max-Min)/ Min	+31%	+300%	+300%	+100%	+67%	+7%	+9%	+200%	+5%
% Change in Loss (LSB)	+150%	-23%	+44%	+29%	-10%	-32%	0%	+14%	-20%
% Change in Input Noise T_M(LSB)	+14%	-40	+84%	+130%	+58%	+55%	-43%	-14%	+47%
% Change in Output Noise (t_r x290)	-14%	+15%	0%	+12%	+18%	+38%	-23%	-11%	+30%
% Change in IF Mismatch $\lvert\Gamma\rvert=\frac{VSWR-1}{VSWR+1}$	-33%	-39%	+11%	-13%	-4%	+12%	+1%	-5%	+8%

Fig. 12. A table summarizing the effects of nine diode parameters on the performance of the 180-GHz mixer. The numbers show whether an increase in the particular diode parameter increases (+) or decreases (−) the mixer conversion loss (LSB), equivalent input noise temperature (LSB), output noise temperature ($t_r \times 290$), and VSWR at the IF port (referred to 50 Ω). The last four parameters in the table, η, ϕ_{bi}, i_s, and T, are not independently variable in practice, so care should be used in interpreting their sensitivities (see text).

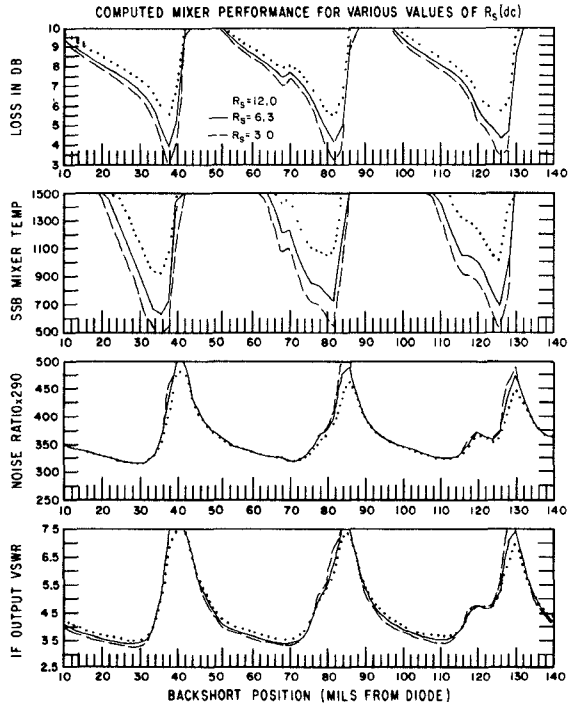

Fig. 13. The computed mixer performance at 180 GHz when R_s(dc) = 3, 6.3, and 12 Ω. In the top two graphs, only the lower sidebands are compared (R_s = 6.3 is our standard value).

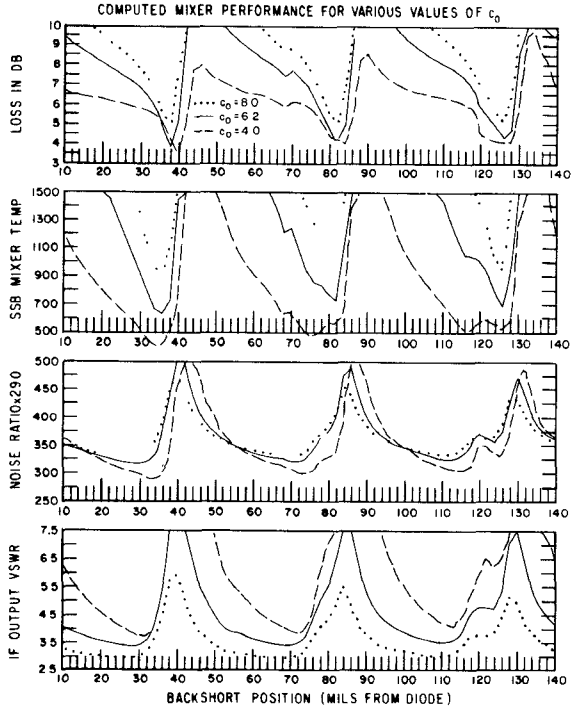

Fig. 14. The computed mixer performance at 180 GHz when c_0 = 4, 6.2, and 8 fF. In the top two graphs, only the lower sidebands are compared (c_0 = 6.2 fF is our standard value).

$R_s(dc)$: Considerable effort has been made in trying to reduce the diode series resistance as much as possible. The series resistance most strongly affects the thermal noise component and the conversion loss; however, a fairly substantial change in $R_s(dc)$ is required to obtain any significant improvement in mixer performance. Fig. 13 shows the change in mixer performance when R_s is varied by a factor of two from its nominal value of 6.3Ω.

c_0: The zero-bias capacitance is one physical parameter which is relatively simple to alter and, as shown in Fig. 14, it has a very strong effect on the mixer performance. The decrease in conversion loss and noise temperature from a 30-percent drop in capacitance more than makes up for any increase in series resistance which might result from using a smaller area diode.

γ: A decrease in the capacitance law exponent most strongly affects the mixer noise temperature, as can be seen in the plots of Fig. 15 ($\gamma = 0$ corresponds to a diode with a constant capacitance equal to c_0). In all instances studied, a decrease in γ improved the mixer noise performance (however, this is not to say that a constant capacitance diode always gives better mixer performance; see, for example, [5, appendix 4]).

η: When changed on its own, the diode ideality factor has a strong effect on the mixer performance. Varying η while i_s is held constant is equivalent to rotating the

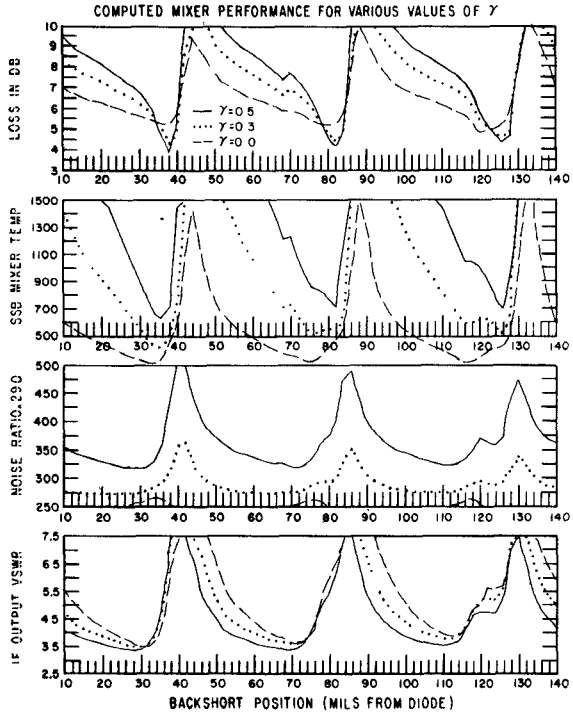

Fig. 15. The computed mixer performance at 180 GHz when $\gamma = 0.0$, 0.3, and 0.5. In the top two graphs, only the lower sidebands are compared ($\gamma = 0.5$ is our standard value).

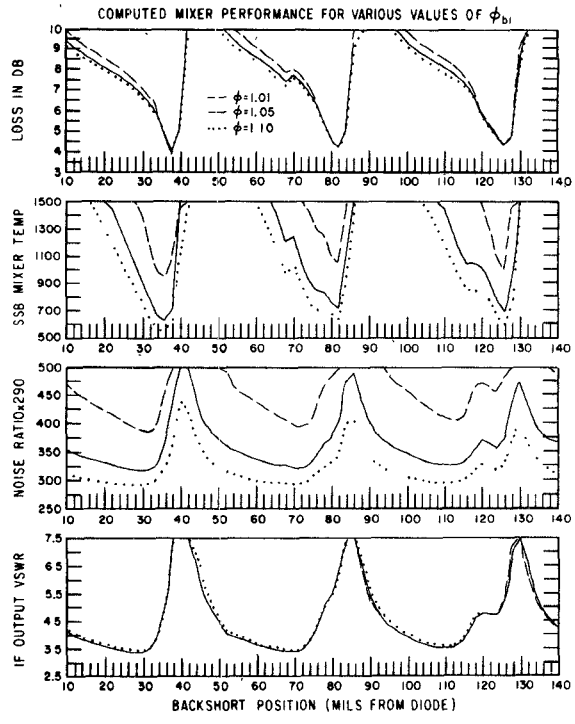

Fig. 17. The computed mixer performance at 180 GHz when $\phi_{bi} = 1.01$, 1.05, and 1.1 V. In the top two graphs, only the lower sidebands are compared ($\phi_{bi} = 1.05$ V is our standard value).

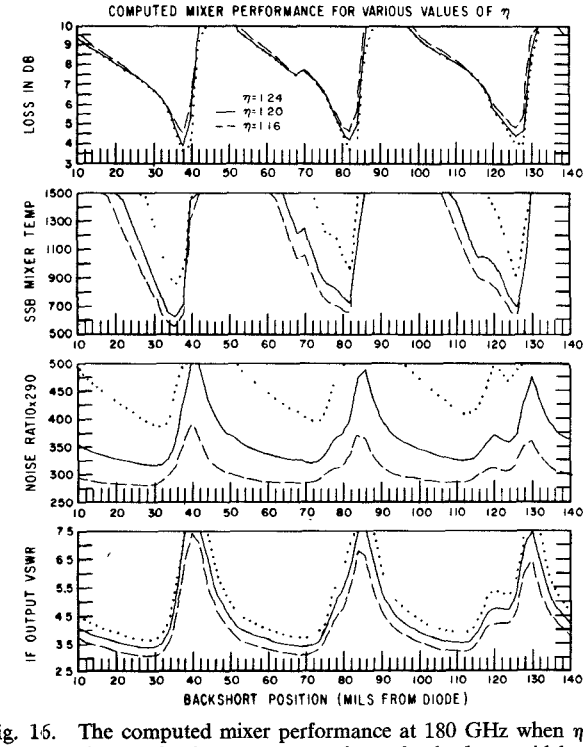

Fig. 16. The computed mixer performance at 180 GHz when $\eta = 1.16$, 1.20, and 1.24. In the top two graphs, only the lower sidebands are compared ($\eta = 1.2$ is our standard value).

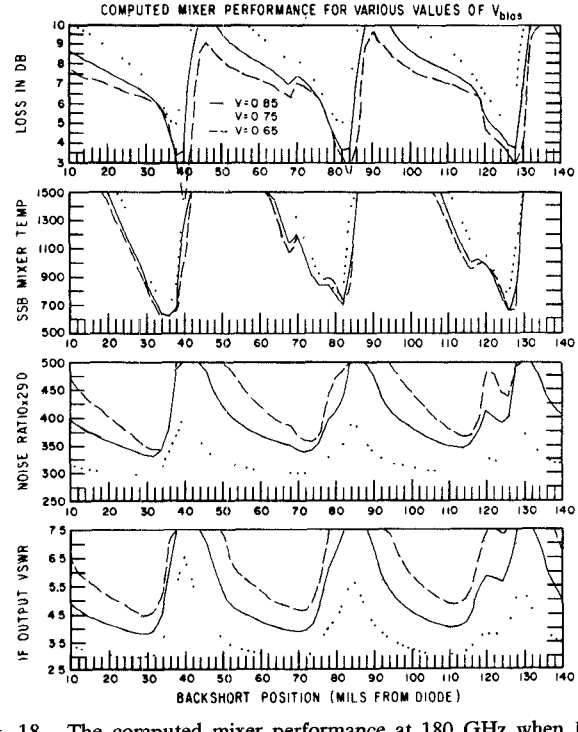

Fig. 18. The computed mixer performance at 180 GHz when $V_{\text{bias}} = 0.65$, 0.75, and 0.85 V. In the top two graphs, only the lower sidebands are compared ($V_{\text{bias}} = 0.80$ V is our standard value).

$\log I$–V curve about its I-axis intercept, and hence, to varying the impedance of the diode at the bias point. Fig. 16 shows the computed mixer performance at 180 GHz when η is varied by ± 3 percent from its nominal value of 1.2. Note that an increase in η requires an increase in the incident LO power if the diode-rectified current is to be maintained at the same level.

In practice, the most likely source of error in specifying η lies in determining its value from the measured $\log I$–V curve. In this case, an error in η is usually accompanied by a corresponding error in the value of i_s (obtained by extrapolation of the $\log I$–V curve back to the I-axis). The effect is equivalent to rotating the $\log I$–V curve about some point in the range of measured values. Using $\eta = 1.16$

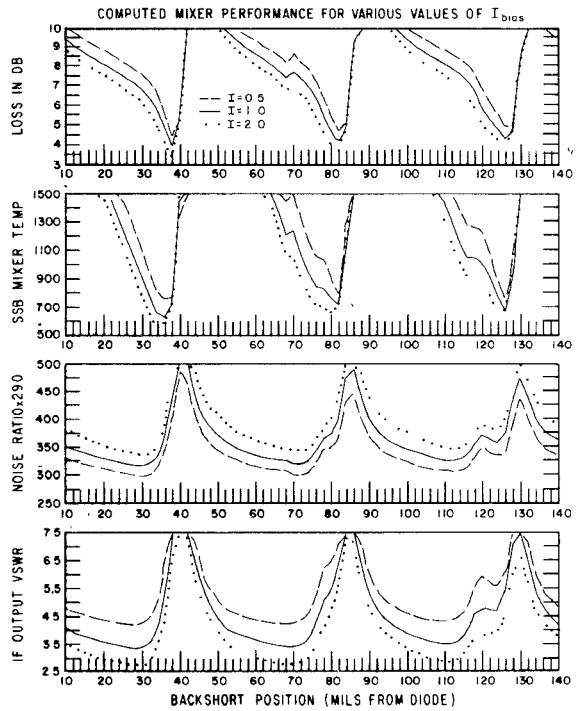

Fig. 19. The computed mixer performance at 180 GHz when $I_{\text{bias}} = 0.5$, 1, and 2 mA. In the top two graphs, only the lower sidebands are compared ($I_{\text{bias}} = 1$ mA is our standard value).

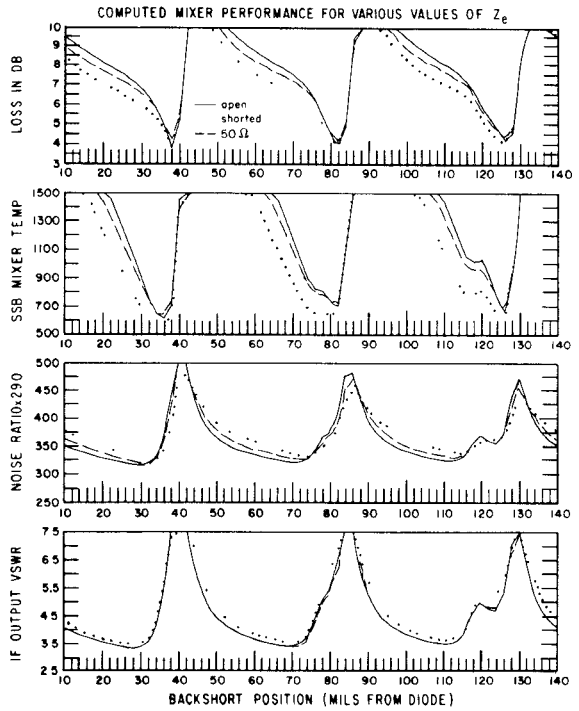

Fig. 20. The computed mixer performance at 180 GHz when the embedding impedances above the upper sideband are (a) open-circuited, (b) short-circuited, and (c) set to 50 Ω. In the top two graphs, only the lower sidebands are compared. Curves *a* are indistinguishable from the standard run (Fig. 11).

and $i_s = 1.52 \times 10^{-17}$ A (instead of 3.77×10^{-17} A) in the computer program, i.e., rotating our diode $\log I$–V curve about the $I = 10$ μA point, caused no noticeable change in mixer performance. This implies that small errors in the measurement of the I–V curve have little effect on the accuracy of the mixer analysis, as the error in slope (η) will be compensated for by the variation in the $\log I$-axis intercept (i_s).

ϕ_{bi}: The built-in potential becomes an important parameter when the voltage across the diode swings close to ϕ_{bi} at some point during the LO cycle, causing the depletion layer capacitance to become very large. When this occurs, the noise temperature of the mixer is the most affected parameter (increasing substantially as the peak value of v_d gets very close to ϕ_{bi}). At other operating points, ϕ_{bi} acts inversely with η, however, with a less pronounced effect. Fig. 17 contains plots of the mixer performance when ϕ_{bi} is varied by ± 5 percent from its nominal value of 1.05. The lowest value of the built-in potential shown in the figure (1.01) corresponds to an operating point at which the maximum value of v_d in an LO cycle is 99.3 percent of ϕ_{bi}.

i_s: Changing the saturation current while η and ϕ_{bi} remain fixed is equivalent to a shift of the diode $\log I$–V curve along the V axis. Curves showing the effects of a 50-percent change in i_s are given in [5].

T: Varying the diode temperature, while i_s remains fixed (physically quite impractical), has the same effect as a proportional change in η (see [5] for plots).

GISSMIX can also be used to search for the optimum diode operating point, that is, the combination of dc bias and rectified current which results in the best mixer performance. These quantities are limited by the available LO power and also by the power-handling capacity of the diode.

Fig. 18 shows the computed mixer performance at 3 different dc-bias voltage settings (in each case, the diode rectified current is 1 mA). The mixer noise and loss decrease with the bias voltage (the loss actually falls below 3 dB at some points due to parametric effects); however, the available LO power is increasing substantially (4 mW at 0.65 V compared to 0.6 mW at 0.8 V).

In Fig. 19 the dc bias current is varied from 0.5 to 2.0 mA. Here, we find that increasing the rectified current in the diode, by increasing the LO power, results in improved mixer performance.

We have also looked at the effects of the higher harmonic terminations on the mixer performance. The graphs in Fig. 20 show the computed mixer performance at 180 GHz when the embedding impedances Z_e (outside R_s) above the upper sideband are a) open-circuited, b) short-circuited, and c) set to 50 Ω. The open-circuited results (curves *a*) in Fig. 20) are identical to those obtained when we use our measured values of Z_e in the computer program. If we compare our actual mixer to one in which the higher harmonic impedances are short circuits (curves *b* in Fig. 20), we see that we cannot make the usual assumption that the diode capacitance shorts out the higher harmonics without introducing noticeable errors in the predicted performance. Subsequent analysis showed, however, that, in our mixer, short-circuiting the sideband impedances above the second harmonic (364 GHz) had no significant effect,

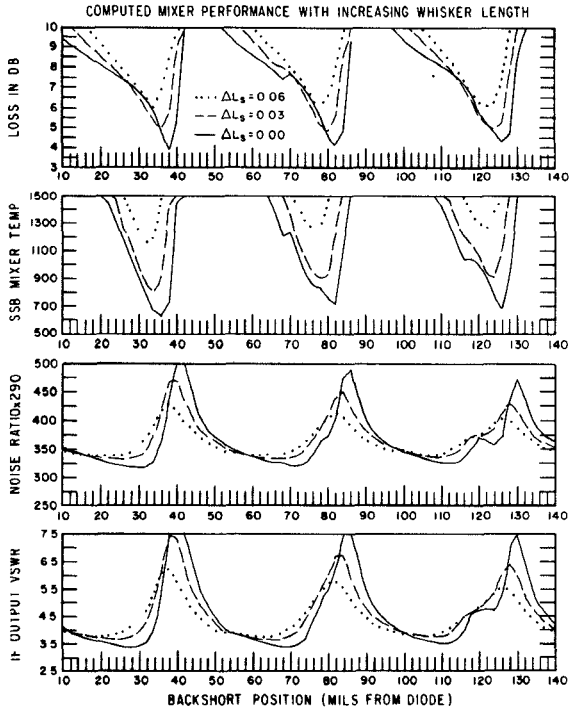

Fig. 21. The computed mixer performance at 180 GHz when the diode contact whisker length is increased ($\Delta L_s = 0.0$, 0.03, and 0.06 nH). In the top two graphs, only the lower sidebands are compared ($\Delta L_s = 0.0$ is our standard value).

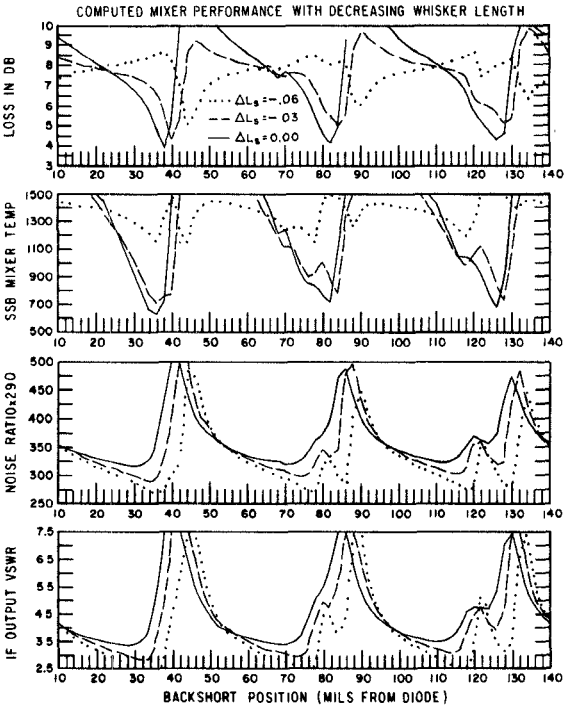

Fig. 22. The computed mixer performance at 180 GHz when the diode contact whisker length is decreased ($\Delta L_s = 0.0$, -0.03, and -0.06 nH). In the top two graphs, only the lower sidebands are compared ($\Delta L_s = 0.0$ is our standard value).

and it is probably fair to assume that, for most analyses, only the first 4 LO harmonics[3] (ω_p, $2\omega_p$, $3\omega_p$, and $4\omega_p$) and the first two harmonic sideband pairs ($\omega_p \pm \omega_{IF}$ and $2\omega_p \pm \omega_{IF}$) need be considered.

In optimizing a diode mounting structure, it is not generally possible to adjust the impedance at each harmonic independently. One physical parameter which can be changed easily is the length of the diode contact whisker. Increasing the whisker length is approximately equivalent to adding an inductance in series with the measured embedding impedances. This situation is examined in Fig. 21, where the 180-GHz mixer performance is compared when 0.03 and 0.06 nH are added in series with the measured embedding impedances (adding 0.03 nH to Z_e is approximately equivalent to a 0.001-in increase in whisker length). Fig. 22 shows the results of removing 0.03 and 0.06 nH from the measured embedding impedances. The whisker length used in the WR-5 mixer appears to be very close to optimum for this mount.

VIII. Conclusion

The computer program GISSMIX has been used to analyze a WR-5 mixer with a GaAs Schottky-barrier diode and has shown excellent agreement with measurements at 150 and 180 GHz. The results indicate that at room temperature and at least up to 200 GHz, the current-transport processes in these diodes can be described accurately by the thermionic emission theory. The high-frequency effects (charge carrier inertia, dielectric relaxation, and plasma resonance [14]), which are significant at the higher harmonics, have no noticeable effect on the mixer. Nor have we observed any contributions from intervalley and/or lattice scattering or hot electron noise. Our results emphasize the need for separate sideband measurements at the signal and image frequencies, and point out the necessity for characterizing the diode mount up to at least the second harmonic sideband frequency and the fourth harmonic of the LO. The sensitivity analysis shows the diode parameters which have the most effect on the mixer performance. We have also seen how the whisker length can be used to optimize the mixer performance for a particular diode and mounting structure.

It would not be fair to generalize the results presented in this paper in an attempt to direct the course of future mixer development. What we can do is offer the mixer designer a tool which can be used i) to determine the optimum diode parameters for a particular mount, or ii) to construct a mount which optimizes the impedances seen by a particular diode. By performing an extensive analysis, such as that presented in this paper, it is possible to study the effects of a wide variety of parameters and ultimately use them to produce better mixers.

[3]Although the third and fourth LO harmonic impedances have no discernible effect on the mixer large-signal behavior, they are used in the computer analysis to derive the second harmonic sideband terms of the small-signal admittance matrix, which must not be set arbitrarily as this can correspond to nonphysical situations [19].

Acknowledgment

The authors would like to thank Dr. R. J. Mattauch and G. Green at the University of Virginia, Charlottesville, for kindly supplying the diodes which have enabled us to

obtain such excellent performance from our WR-5 mixer, Dr. J. A. Archer at the National Radio Astronomy Observatory for his help on the design of a WR-5 frequency multiplier which we used as part of our signal source for the mixer conversion loss measurements, and J. A. Grange, H. Miller, and I. Silverberg for fabricating the mixer, waveguide components, and scale model.

REFERENCES

[1] P. H. Siegel and A. R. Kerr, "Computer analysis of microwave and millimeter-wave mixers,"*IEEE Trans. Microwave Theory Tech.*, vol. MTT-28, pp. 275–276, Mar. 1980.

[2] A. R. Kerr, R. J. Mattauch, and J. A. Grange, "A new mixer design for 140-220 GHz," *IEEE Trans. Microwave Theory Tech.*, vol. MTT-25, pp. 399–401, May 1977.

[3] D. N. Held and A. R. Kerr,"Conversion loss and noise of microwave and millimeter-wave mixers: Part I—Theory," and "Part II—Experiment," *IEEE Trans. Microwave Theory Tech.*, vol. MTT-26, pp. 49–61, Feb. 1978.

[4] A. R. Kerr, "A technique for determining the local oscillator waveforms in a microwave mixer," *IEEE Trans. Microwave Theory Tech.*, vol. MTT-23, pp. 828–831, Oct. 1975.

[5] P. H. Siegel, "Topics in the optimization of millimeter-wave mixers," Ph.D. dissertation, Columbia University, New York, NY, Oct. 1983. Published as NASA Tech. Paper 2287, National Aeronautics and Space Administration, Washington, DC, Mar. 1984.

[6] W. K. Gwarek, "Nonlinear analysis of microwave mixers," M. S. thesis, Mass. Institute of Tech., Cambridge, MA, Sept. 1974.

[7] R. G. Hicks and P. J. Khan, "Numerical analysis of nonlinear solid-state device excitation in microwave circuits," *IEEE Trans. Microwave Theory Tech.*, vol. MTT-30, pp. 251–259, Mar. 1982.

[8] H. C. Torrey and C. A. Whitmer, *Crystal Rectifiers*. New York: McGraw-Hill, MIT Radiation Laboratory Series vol. 15, 1948.

[9] R. L. Eisenhart and P. J. Khan, "Theoretical and experimental analysis of a waveguide mounting structure," *IEEE Trans. Microwave Theory Tech.*, vol. MTT-19, pp. 706–719, Aug. 1971.

[10] S. M. Sze, *Physics of Semiconductor Devices*. New York: Wiley, 1969.

[11] F. A. Padovani and R. Stratton, "Field and thermionic-field emission in Schottky barriers," *Solid-State Electron.* (GB), vol. 9, pp. 695–707, 1966.

[12] B. Pellegrini and T. Di Leo, "Intervalley scattering effect on the current–voltage characteristic of GaAs-metal contacts," *Alta Frequenza*, vol. 46, no. 8, pp. 345–353, Aug. 1977.

[13] W. R. Frensley, "High frequency effects of ballistic electron transport in semiconductors," *IEEE Electron Device Lett.*, vol. EDL-1, no. 7, pp. 137–139, July 1980.

[14] K. S. Champlin and G. Eisenstein, "Cutoff frequency of submillimeter Schottky-barrier diodes," *IEEE Trans. Microwave Theory Tech.*, vol. MTT-26, pp. 31–34, Jan. 1978.

[15] R. J. Mattauch, private communication.

[16] S. Weinreb and D. R. Decker, private communication, as described in detail in [3].

[17] L. E. Dickens, "Spreading resistance as a function of frequency," *IEEE Trans. Microwave Theory Tech.*, vol. MTT-15, pp. 101–109, Feb. 1967.

[18] S. Weinreb and A. R. Kerr, "Cryogenic cooling of mixers for millimeter and centimeter wavelengths," *IEEE J. Solid State Circuits*, vol. SC-8, no. 1, pp. 58–63, Feb. 1973.

[19] A. R. Kerr, "Noise and loss in balanced and sub-harmonically pumped mixers: Part II—Application," *IEEE Trans. Microwave Theory Tech.*, vol. MTT-27, pp. 944–950, Dec. 1979.

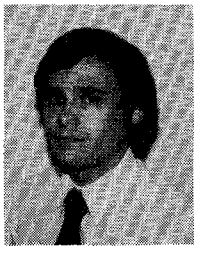

Peter H. Siegel (S'78–M'83) was born in New Rochelle, NY, in 1954. He received the B.A. degree from Colgate University in 1976 and the M.S. and Ph.D. degrees in electrical engineering from Columbia University in 1978 and 1983, respectively.

From 1975 to 1983, he was a Research Assistant at the NASA/Goddard Institute for Space Studies in New York, where he worked on the analysis of millimeter-wave Schottky-diode mixers. In October 1983, he began a one year tenure as a NASA/National Research Council Associate, to develop submillimeter-wave antennas and mixers. Dr. Siegel will be joinging the National Radio Astronomy Observatory in Charlottesville, VA, in December 1984, where he expects to continue working on low-noise millimeter and submillimeter-wave receivers.

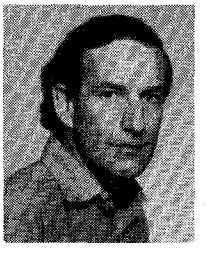

Anthony R. Kerr (S'64–A'66–SM'78–F'84) was born in England on August 30, 1941. He received the B.E., M.Eng.Sc., and Ph.D. degrees from the University of Melbourne, Australia, in 1964, 1967, and 1969, respectively.

In 1969, he joined the Commonwealth Scientific and Industrial Research Organization, Sydney, Australia, to work on low-noise receivers for radio astronomy. From 1971 to 1974, he worked at the National Radio Astronomy Observatory, Charlottesville, VA, developing cryogenically cooled Schottky-diode mixer receivers for millimeter-wavelength radio astronomy. Between 1974 and 1984, he developed Schottky, Josephson, and SIS millimeter-wave receivers at the NASA/Goddard Institute for Space Studies, New York, NY. In 1984, he returned to the National Radio Astronomy Observatory, where he is doing research on low-noise millimeter-wave systems.

Dr. Kerr is a member of URSI Commission J and the Astronomical Society of Australia. He was co-recipient of the 1978 IEEE Microwave Prize, and received the 1983 NASA Exceptional Engineering Achievement Medal.